Jurnal Media Mesin, Vol. 24 No. 2
Printed ISSN: 1411-4348
Online ISSN: 2541-4577

EFFECT OF STAINLESS STEEL 304 TIG WELDING AMPERE ON STRESS CORROSION CRACKING PHENOMENON

Moch Chamim
Mechanical Engineering
Sekolah Tinggi Teknologi "Warga" Surakarta
Email: chamim@sttw.ac.id

Farit Ardiyanto
Electrical Engineering
Sekolah Tinggi Teknologi "Warga" Surakarta
Email: farit@sttw.ac.id

ABSTRAK

Artikel ini membahas hasil eksperimen baja tahan karat tegangan retak tegangan grade 304 setelah pengelasan GTAW dengan simulasi korosi lingkungan. Fenomena korosi yang terjadi adalah Stress Corrosion Cracking (SCC). Metode eksperimen berupa spesimen yang dilas menggunakan arus masing-masing 55, 60, dan 65 Ampere dengan laju aliran gas pelindung argon 5 L/menit. Beban tarik konstan 2000 N dan 4000 N dalam keadaan benda uji direndam selama 2 x 24 jam dalam larutan HCl + Aquades. Parameter laju alir Ampere dan shielding gas yang berbeda mempengaruhi fenomena retakan. Kekerasan dan Struktur Mikro Vickers digunakan untuk mengevaluasi area las. Ampere lasan terendah menghasilkan retakan kasar maksimum dari permukaan dan terlihat di permukaan. Meningkatnya kekerasan benda uji arus 55 Ampere menunjukkan adanya perubahan struktur atau fasa setelah dilakukan pengelasan. Ampere tertinggi menghasilkan retakan halus di semua permukaan.

Kata kunci: stainless steel 304, korosi, SCC, TIG.

ABSTRACT

This article discusses the experimental results of stress corrosion cracking grade 304 stainless steel after GTAW welding under environmental corrosion simulation. The corrosion phenomenon that occurs is Stress Corrosion Cracking (SCC). The experimental method is a specimen welded using a current of 55, 60, and 65 Ampere respectively with a gas flow rate of 5 L/min argon shielding gas. The constant tensile loads of 2000 N and 4000 N in the state of the test object immersed for 2 x 24 hours in a solution of HCl + Aquades. Different Ampere and shielding gas flow rate parameters affected the cracks phenomenon. Vickers Hardness and Microstructure were used to evaluate the weld area. The lowest ampere of the weld results in maximum rough cracks from the surface and it's visible on the surface. The increased hardness of the 55 Ampere current specimen indicates a change in structure or phase after welding. The highest ampere produces fine cracks on all surfaces.

Keywords: *stainless steel 304, corrosion, SCC, TIG.*

1. INTRODUCTION

Steel is one of the groups of engineering materials that have a reasonably high strength and resistance. One type of steel is stainless steel which has special properties of resistance to corrosive, so it is often called stainless steel. The type of stainless steel commonly used in the industrial world is type 304, which is included in the austenitic Stainless-Steel class. This type of Stainless Steel is widely used in the food industry and structures for construction and is also needed by factories because it has weldable properties. In the food industry, Stainless Steel type 304 is widely used to manufacture conveyors, piping, and storage tanks.

Stainless steel material, under certain conditions as a result of the manufacturing process, especially welding, will change its basic structure. Corrosive environmental loads and conditions trigger material failures that give rise to cracks. The combination of load and corrosive on the material is called Stress Corrosion Cracking (SCC). The emergence of cracks on the surface of the material identifies SCC. Then over time, the cracks spread, failing a material or construction. The emergence of SCC will reduce the life of the structure that has been made.

The decrease in corrosion resistance of type 316 stainless steel due to the welding process starting from the grain boundary of the surface section and then into cracked propagation along the grain boundary has been studied by several researchers [1]–[3]. In addition, residual stress is also the main factor for forming cracks [4][5]. The residual stress appears after the welding process due to the influence of heat in the material. This will

increase the material's burden and accelerate the emergence of SCC [6]. Welding parameters, especially amperes and welding speed, significantly affect penetration so that it impacts the area around welding [7][8].

Other studies have stated that pitting corrosion causes a vulnerability to the occurrence of defects which become the initiation of cracks or cracks. Pitting corrosion starts from the surface in certain positions due to the non-uniformity of the protective layer. This phenomenon is known as Redox (Reduction Oxidation) and occurs in small holes on the surface when metal is immersed in liquid [9]. Several manipulation models are used with experimental methods [10][11] and simulation models [12][13] to study pitting corrosion behavior on material surfaces.

This study aims to determine the number and length of cracks that occur in the stainless-steel welding area, especially type 304. The data are obtained to determine the character of cracks due to the phenomenon of SCC on stainless steel materials after welding. Thus, manufacturing failures due to stainless steel welding can be predicted earlier.

2. METHODOLOGY

2.1 Materials and Specimen Preparation

The material used is type 304 stainless steel with a thickness of 3 mm. Welding uses Tungsten Inert Gas (TIG) with ER308L filler with a diameter of 2.4 mm and Argon (Ar) as a shielding gas at a speed of 5 L/minute. Variations in welding currents of 55, 60, and 65 Amperes are used to differentiate the amount of heat energy during welding. The microstructure test used HNO_3 20 ml, HCl 10 ml, and Aquades 30 ml to determine the morphology of the welding results. The Vickers hardness test with a load of 0.98 N starts from the weld metal to the base metal to determine the hardness distribution in the welding area. Specimens were shaped according to ASTM E8 standards for tensile strength and SCC testing. Specimen labeling according to Amperage is 55 A 5Ar, 60 A 5Ar, and 65 A 5Ar respectively.

Figure 1. Specimen conditions during SCC testing

2.2 SCC Test

The SCC load value is below the average maximum tensile loading result of 23.086 N. Before the SCC test, a tensile test is carried out to get the maximum load. Tensile testing of 3 specimens for each parameter was then averaged, as shown in Table 1.

Table 1. Average tensile testing

Current	Gases Flow	to	Bo	Ao	F_{max}	σ_{max}
(Ampere)	(L/min)	(mm)	(mm)	(mm^2)	(N)	(N/mm^2)
55	5	3	12.3	36.9	23.067	620.23
60	5	3	12.2	36.6	21.630	570.96
65	5	3	12.7	38.1	24.560	647.97
				Average	23.086	613.05

Specimens were immersed, as shown in Figure 1. in a mixture of 5 ml HCl solution and 20 ml distilled water for 24 hours. During immersion, the specimens were given a constant load for two tests using 2000 N and 4000 N loads, as shown in Figure 2. So, the total SCC testing time was 2 x 24 hours. After the SCC test, the

specimen in the welding area as shown in Figure 3. The top (caping) and bottom (root) crack character was observed.

Figure 2. Equipment of SCC test

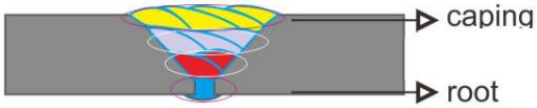

Figure 3. Target area of SCC analysis

3. RESULTS AND DISCUSSION

3.1 Hardness Test

Hardness testing uses the Vickers test method to know hardness distribution, especially in welding. The highest hardness is found in the 55A 5Ar specimen in the area between HAZ and Weldmetal, as shown in Figure 3. This is due to the carbon element bonding with the chromium during the cooling process. Chromium and carbon are bonded to form chromium carbide, which has a higher hardness than the base material. This causes chromium to experience a decrease in its function as a corrosion resistant agent because the film layer is not formed. Violence can also trigger cracks due to its brittle nature. The hardness of the weld metal region has a low value because this area experiences high heat and rapid cooling, so there was not enough time for the carbon to bond with the chromium.

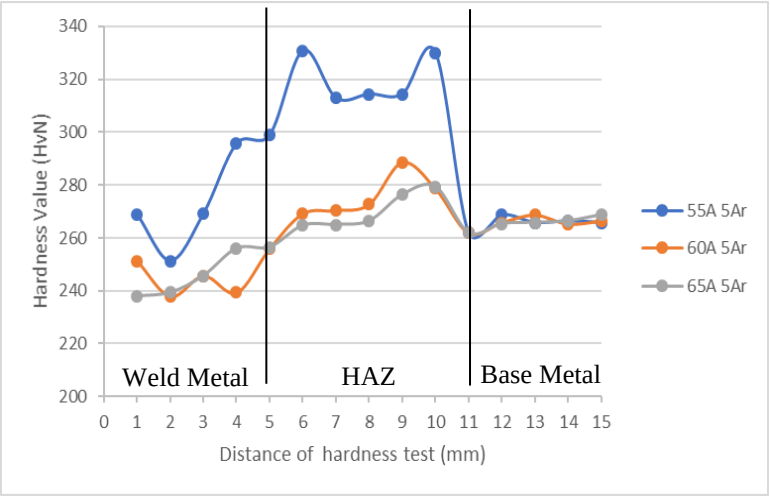

Figure 4. The Hardness value of the welding area

3.2 Morphology of SCC

SCC specimen test results were taken using a microstructure magnification of 50X in several unified parts.

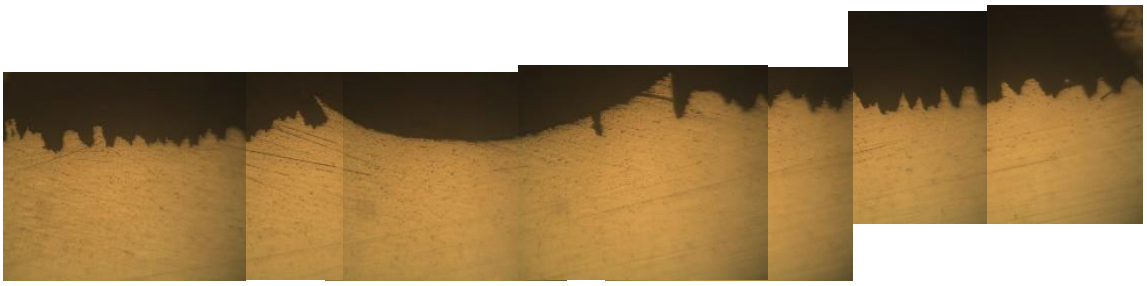

(a)

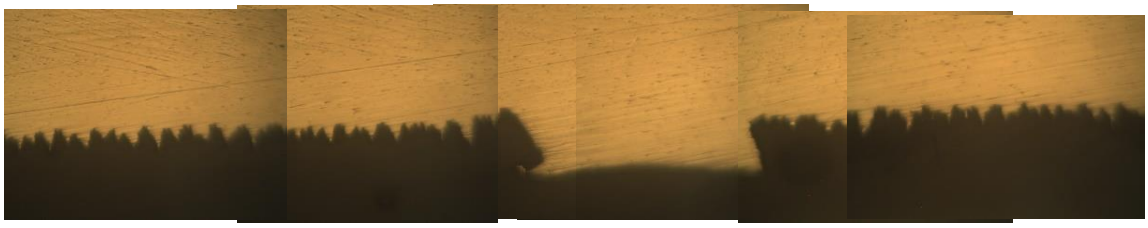

(b)

Figure 5. Corrosion surface form of specimen 55A 5Ar caping (a) and root (b) region

The 55A 5Ar specimen was corroded in both parts of the target area, as shown in Figures 5(a) and 5(b). It can be seen that the corrosion that occurs is extreme because the film layer in this area is susceptible. Corrosion occurs throughout the surface. This strengthens the analysis of hardness where there is an increase in hardness due to the formation of chromium carbides were chromium.

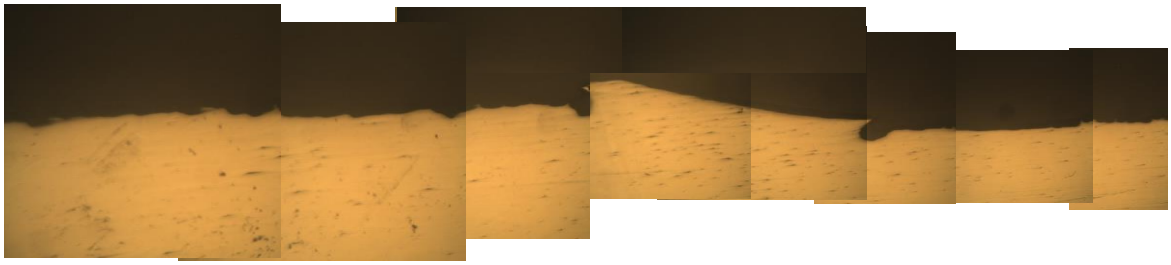

(a)

(b)

Figure 6. Corrosion surface form of 60A 5Ar caping (a) and root (b) region

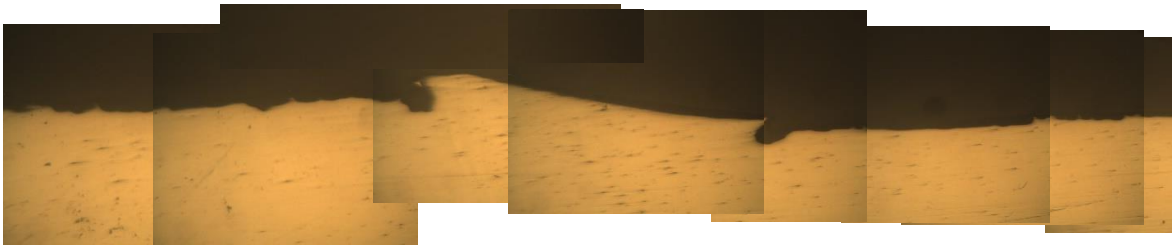

(a)

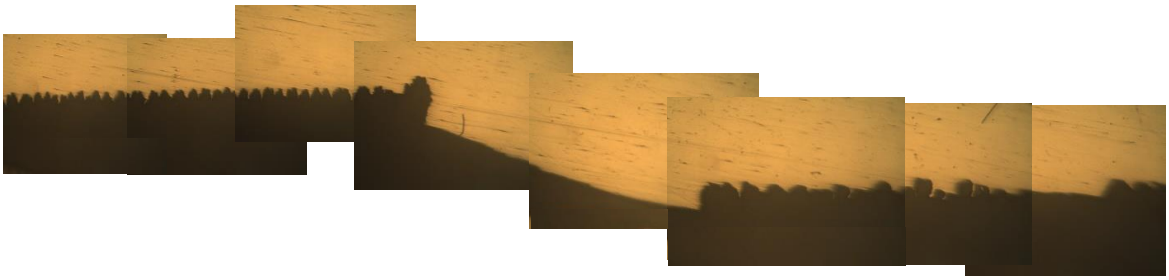

(b)

Figure 7. Corrosion surface form of 65A 5Ar caping (a) and root (b) region

Resistance to corrosion is noticeable by the addition of the magnitude of the welding ampere value. Specimens of 60A 5Ar *caping* parts such as Figure 5(a) corrosion occur very little. Surface corrosion does not have a significant impact because this part is film protected. However, the area between *weld metal* and HAZ corrosion occurs due to large voltages occurring in the grain binding in this area. The root surface of *specimen* 60A 5A looks very corrosive as Figure 6(b). The same phenomenon occurs in 65A 5Ar specimens where corrosion resistance looks good as Figure 7(a). The interesting thing about the *root* of the 65A 5Ar specimen is that the cracks that occur are so smooth. This indicates a longer corrosion hold of the surface part so that the surface reduction is only a little bit.

4. CONCLUSION

The results of the study can be concluded about the effect of SCC on stainless steel 304 material:

1. Ampere affects corrosive resistance, where heat energy can change chromium to chrome carbide. The results of the study can be concluded about the effect of SCC on stainless steel 304 material;
2. The hardness value can be used as a reference for changes in the structure of the welding area;
3. The heat energy will affect the root, where the part undergoes structural changes due to welding.

ACKNOWLEDGMENTS

The author is very grateful to Kemenristek/BRIN in funding of Hibah Nasional Skema Penelitian Dosen Pemula (PDP) with a research contract 1/064026/PG/SP2H/TD/2021.

REFERENCES

[1] Anon, “Corrosion of Stainless Steels.,” *Eng.*, vol. 218, no. 11, pp. 1207–1209, 1978, doi: 10.1016/B978-0-12-803581-8.02893-9.

[2] J. Xin, Y. Song, C. Fang, J. Wei, C. Huang, and S. Wang, “Evaluation of inter-granular corrosion susceptibility in 316LN austenitic stainless steel weldments,” *Fusion Eng. Des.*, vol. 133, no. September 2017, pp. 70–76, 2018, doi: 10.1016/j.fusengdes.2018.05.078.

[3] X. Li, J. Liu, J. Sun, X. Lin, C. Li, and N. Cao, “Effect of microstructural aspects in the heat-affected zone of high strength pipeline steels on the stress corrosion cracking mechanism : Part I . In acidic soil environment,” *Corros. Sci.*, no. June, p. 108167, 2019, doi: 10.1016/j.corsci.2019.108167.

[4] L. Dong, Q. Peng, E. Han, W. Ke, and L. Wang, “Stress Corrosion Cracking in the Heat Affected Zone of a Stainless Steel,” *Eval. Program Plann.*, 2016, doi: 10.1016/j.corsci.2016.02.030.

[5] W. Chung, J. Huang, L. Tsay, and C. Chen, “Stress corrosion cracking in the heat-affected zone of A508

steel welds under high-temperature water," *J. Nucl. Mater.*, vol. 408, no. 1, pp. 125–128, 2011, doi: 10.1016/j.jnucmat.2010.10.052.

[6] B. A. Kessal, C. Fares, M. H. Meliani, A. Alhussein, O. Bouledroua, and M. François, "Effect of gas tungsten arc welding parameters on the corrosion resistance and the residual stress of heat affected zone," *Eng. Fail. Anal.*, p. 104200, 2019, doi: 10.1016/j.engfailanal.2019.104200.

[7] B. Singh, P. Singhal, and K. K. Saxena, "Investigation of thermal efficiency and depth of penetration during GTAW process," *Mater. Today Proc.*, vol. 18, pp. 2962–2969, 2019, doi: 10.1016/j.matpr.2019.07.166.

[8] Z. Chen, J. Chen, and Z. Feng, "Welding penetration prediction with passive vision system," *J. Manuf. Process.*, vol. 36, no. October, pp. 224–230, 2018, doi: 10.1016/j.jmapro.2018.10.009.

[9] F. J. Cárcel-Carrasco, M. Pascual-Guillamón, L. S. García, F. S. Vicente, and M. A. Pérez-Puig, "Pitting corrosion in AISI 304 rolled stainless steel welding at different deformation levels," *Appl. Sci.*, vol. 9, no. 16, 2019, doi: 10.3390/app9163265.

[10] Y. Chen, B. Yang, Y. Zhou, Y. Wu, and H. Zhu, "Evaluation of pitting corrosion in duplex stainless steel Fe20Cr9Ni for nuclear power application," *Acta Mater.*, vol. 197, pp. 172–183, 2020, doi: 10.1016/j.actamat.2020.07.046.

[11] E. Arzaghi, B. H. Chia, M. M. Abaei, R. Abbassi, and V. Garaniya, "Pitting corrosion modelling of X80 steel utilized in offshore petroleum pipelines," *Process Saf. Environ. Prot.*, vol. 141, pp. 135–139, 2020, doi: 10.1016/j.psep.2020.05.024.

[12] X. Wang *et al.*, "Pitting corrosion of 2Cr13 stainless steel in deep-sea environment," *J. Mater. Sci. Technol.*, 2020, doi: 10.1016/j.jmst.2020.04.036.

[13] L. Feng *et al.*, "A parametric study on effects of pitting corrosion on steel plate's ultimate strength," *Appl. Ocean Res.*, vol. 95, no. December 2019, p. 102026, 2020, doi: 10.1016/j.apor.2019.102026.